CHINESE JOURNAL OF PHYSICS VOL. 35, NO. 3 OCTOBER 1997

Electrical Conduction of $Tl_{20}Ge_{14}Se_{66}$

N. M. Megahid, A. M. Ahmed, and M. M. Ibrahiem
Physics Department, Faculty of Science, Sohag, Egypt
(Received January **16, 1997**)

For bulk samples of the quenched $Tl_{20}Ge_{14}Se_{66}$ either as-prepared or isochronically annealed for one hour at different temperatures up to 150 °C, the current-voltage characteristics at different temperatures of measurements (T) and of annealing (T_{an}) were non-linear especially when the applied potential difference exceeds certain value which is dependent on both T and T_{an}. The field dependence of the current denity could be described by an empirical power equation. The field enhancement of the electrical conductivity followed an exponential equation. The temperature dependent characteristic length $a(T)$ possessed maximum value at certain values of T and T_{an}, and becomes lower by about one order of magnitude by annealing. Annealing in the range (100-130 °C) was associated with appearance of semimetallic behaviour which characterized the relatively low range of T. Semimetallic-semiconductor transition occurred at particular temperatures depending on that of annealing. Otherwise, semimetallic behaviour extended over the whole range of T. The band to band activation energy changed with the pre-exponential conductivity according to the Meyer-Neldel rule. In the range $T_{an} \leq 90$ °C, Mott's formula for hopping conductivity seemed applicable and the characteristic temperature, the density of the localized states, the average hopping distance and the hopping energy were calculated.

PACS. 72.20.–i– Conductivity phenomena in semiconductors and insulators.
PACS. 72.80.Ng– Disordered solids.

I. Introduction

Studies on the semiconducting chalcogenide glasses of the system TlGeSe have been carried out intensively because of their important optical and electronic applications [1-3]. The electronic properties of the vitreous chalcogenide semiconductors depend more on the local distribution in the atomic arrangement than on the absence of long-range order. During the galss formation, the different bond strength and angles between particular atoms lead to predominant space orientation, i.e, to short-range order with the absence of translation symmetry.

Madhavi Zope et al. [4] found that the room temperature current- voltage characteristics of the $Ge_{10}Se_{90-x}Tl_x$ system, with x = 1 to 9 at. % Tl, are linear for lower voltages and become non-linear at higher voltages. They found also that, the room-temperature conductivity increases with increasing the content of Tl in the compositions. Accordingly, several models have been proposed [5-6] to explain the non-linear behaviour and threshold switching in chalcogenides. However, Madhavi 'Lope et al. [4] explained such nonlinearity

on the basis of the charged defects centers model which was easily proposed by Moruga and Zope [7] to explain the nonlinear current-voltage characteristics in Sb-Se-Te chalcogenides.

Mott and Davis [8] have already described the role of addition of Cu, Ag, Pb and Tl in the Ge-Se and As-Se systems viz. an increase of the electrical conductivity. On the other hand, Madhavi-Zope et al. [4] regarded the increase in the electrical conductivity of Ge-Se system to the addition of Tl which gives more charged defect centers which result in turn in an enhancement of the electrical conductivity. However, through the work of Fritzsche [9], Ovshinsky [10] and Andreev et al. [11], it has been observed that the influence of impurities in chalcogenides is less pronounced than in crystalline materials. To explain this and other phenomena, Mott and Street [12] have assumed that the Fermi level is pinned approximately in the middle of the band gap by charged defect states D^+ and D^-.

Tohge et al. [13] have proved that the different glasses of the system Tl-Ge-Se are having P-type semiconductor behaviour. However, they proposed a two-charge carrier model to explain the obtained results of both electrical and thermoelectric temperature dependence of the composition $Tl_{35}Ge_{20}Se_{45}$. They attributed the small values for the Seebeck coefficient and the activation energy for the thermoelectric power with respect to those for the electrical conductivity as an indication of the increased contribution of electrons to the electrical transport, though holes are still dominant charge carriers.

Throughout this paper we report the current (I) - voltage *(V)* characteristics for as-perpared and annealed bulk samples of the composition $Tl_{20}Ge_{14}Se_{66}$ prepared by the usual melt quenching technique. For the as-prepared condition, the $I-V$ characteristics were measured isothermally in the range $T \leq 80$ °C. For the annealed condition, the characteristics were measured at the end of the period of the isothermal annealing 1 hour at the temperature of annealing itself which was changed in the range $80 \leq T_{an} \geq 150$ °C in steps of 5 °C. Both the field dependence at the different temperatures of measurements and annealng and the thermal activation of the electrical conductivity (σ) were measured. The role of both the environmental and annealing temperatures on the characteristic length, the activation energy and other conduction parameters were revealed.

II. Experimental

The proposed composition $Tl_{20}Ge_{14}Se_{66}$ was prepared from 5N Ge and Tl and 4N Se. The appropriate atomic weight percentages of the three elements were mixed and enclosed in 10 mm ϕ diameter silica tubes sealed under vacuum of the order 10^{-4} torr and then heated in the oven while the temperature was raised continuously to the maximum required value into three steps. First, the temperature of the oven was raised at a rate 3-4 °C/min up to 300 °C and it was kept at this temperature for about 3 hour. Second, the temperature was raised up to 600 °C at the same former rate and then kept at this temperature for 12 hour. Finally, the temperature was raised continuously to about 950 $\pm$ 20 °C, where alloying was performed at this temperature for about 24 hour.

During alloying, the charged silica ampoule was vigorously shaken several times to ensure good mixing of the elements and in turn good homogeneity of the alloy. Quenching was carried out at 0 °C by immersing the tube abruptly into ice cold water.

Strutural investigations were made by means of a Shimatzu X-ray diffractometer unit with $CuK\alpha$ radiation. Samples in power form of an average particle size < 75 $\mu(Micron)$

were prepared for this purpose.

For both the Current (1) - Voltage (V)characteristics and DC electrical conductivity (σ) measurements, samples of thickness $\sim$ 0.275 cm and cross sectional area 0.5 cm^2 were prepared by automatic cutting. The samples having parallel and optically flat surfaces. The contact surfaces were painted with silver paste which was left to dry in vacuum at room temperature. The electrical leads were made of 5N silver wires. A gentle controlled pressure contact sample holder was used for electrical measurements. surements. Further, a simple series electrical circuit was used. The voltage drop across the sample terminals was measured directly by means of 610 °C solid state Electrometer (Keithley). the series current was measured by means of a 177 Micro-Vlot DMM (Keithley). The sensitivity in current and voltage measurements were 10^{-9} $Amp.$ and 10^{-4} V respectively. The environmental temperature (T) was recorded in terms of a precisely calibrated Copper - Constantan thermocouple which was kept very close to the sample surface. The thermocouple junction thermolectric power was measured by means of a Digital multimeter 191 (Keithley) 10^{-6} V. Stabilization in T seems very important, since, measurements were carried out within a relatively narrow range (from room temperature to 150 "C). Thus, fluctuation in temperature was minimized to be less than ± 1°C by means of a standard temperature controller. This was essential for the possibility of isothermal measurements of the $I-V$ characteristics and isothermal and isochronic annealing. Meanwhile, it has to be mentioned that both measurements and annealing have been carried out under vacuum of about 10^{-4} torr.

III. Results and discussion

First of all, as it is seen on the X-Ray diffractogram, Fig. l(a), the as-prepared $Tl_{20}Ge_{14}Se_{66}$ has an amorphous structure.

Despite of annealing at 90oC for lh, the structure was still amorphous Fig. l(b) In contrast, elevating the temperature of annealing (T_{an}) to 116 °C was associated with appearance of weak crytallization peaks at different positions on the diffractogram on Fig. l(c). On the other side, more elevating of the temperature of annealing to 140 °C was associated with both phase separation and more intense crystallization, as shown on Fig. l(d). The separated α-Tl represents the most intense phase and appeared at 28 = 29.689". The directly less intense phase was GeSe which appeared at 26 = 28.69". Tl_2GeSe_3 represents the third intense phase and appeared on the diffractogram at 28 = 30.762". Other Tl-Ge-Se phases with appreciable intensities could be also identified. On the other hand, annealing at 140 oC resulted also in separation of Ge and Se in their elemental forms with appreciable intensities. Moreover, binaries either in the form Ge-Se or $GeSe_2$ were abundant to be identifed. The XRD analysis could draw, in general the conclusion that, the initial (as-prepared composition) $Tl_{20}Ge_{14}Se_{66}$ can not be existed as a stable phase especially at relatively elevated temperature of annealing. Above certain value of T_{an} especially above $T_g \sum$ 110 °C, it dissociates into different intermediate phases in the form of ternaries and binaries with stoichiometery and/or even into the solid state interacting elements Tl, Se and Ge. This makes the study of the effect of the process of annealing on the electrical properties of this material rather complicated.

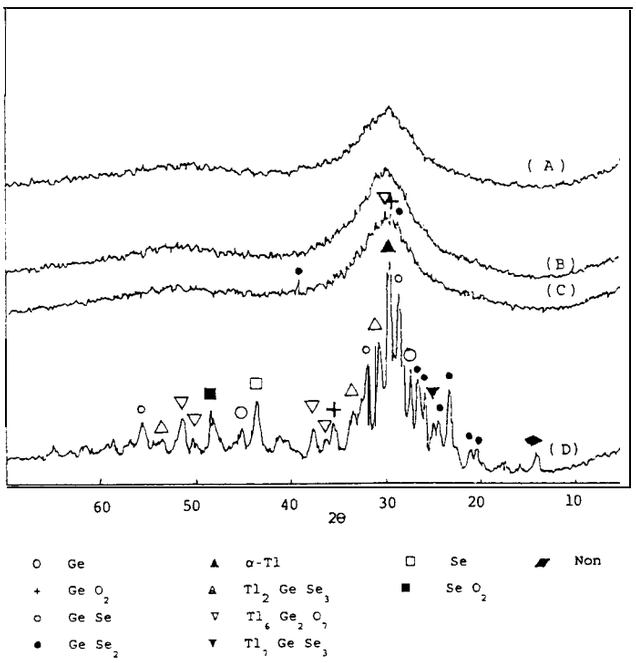

FIG. 1. *X-ray* diffractograms of $Tl_{20}Ge_{14}Se_{66}$ composition at dirrerent conditions: (A) As-perpared, (B) T_{an} = 90 °C, (C) T_{an} = 110 °C and (D) T_{an} = 140 °C.

As shown in Fig. 2(a), the $I-V$ characteristics of bulk as-prepared samples of the composition $Tl_{20}Ge_{14}Se_{66}$ at different fixed temperatures in the range $33 \leq T \leq 80$ °C are consisting of two regions. In agreement with Ref. (4), below a certian applied potential difference, the characteristics are linear and the behaviour is ohmic. Exceeding this potential difference which is dependent on the environmental temperature, the characteristics deviate slightly toward non-ohmic behaviour. However, the conductivity increases with T emphasizing the possibility of thermal actvation of the corresponding electrical conductivity. For the non-ohmic region of the characterictics, the double logarithmic relations of the current density (J) and the applied field (E) were all linear even when the applied electric field was raised to about 350 V/cm (plots which are not shown here as a matter of conciseness). This reveals that, the current density dependence on the applied electric field can, in general, be described by the following empirical power equation

$$J = CE^{n}. \tag{1}$$

The least square fits on ln(J) *vs* $\ln(E)$ plots gave values for the power n plotted as a function of (T) in Fig. 2(c) which deviates slighly from unity characterizing ohmic conduction and almost independent on the temperature of measurements. This slight deviation from unity which seems contradictory to the characteristics on Fig. 2(a) especially at relatively high

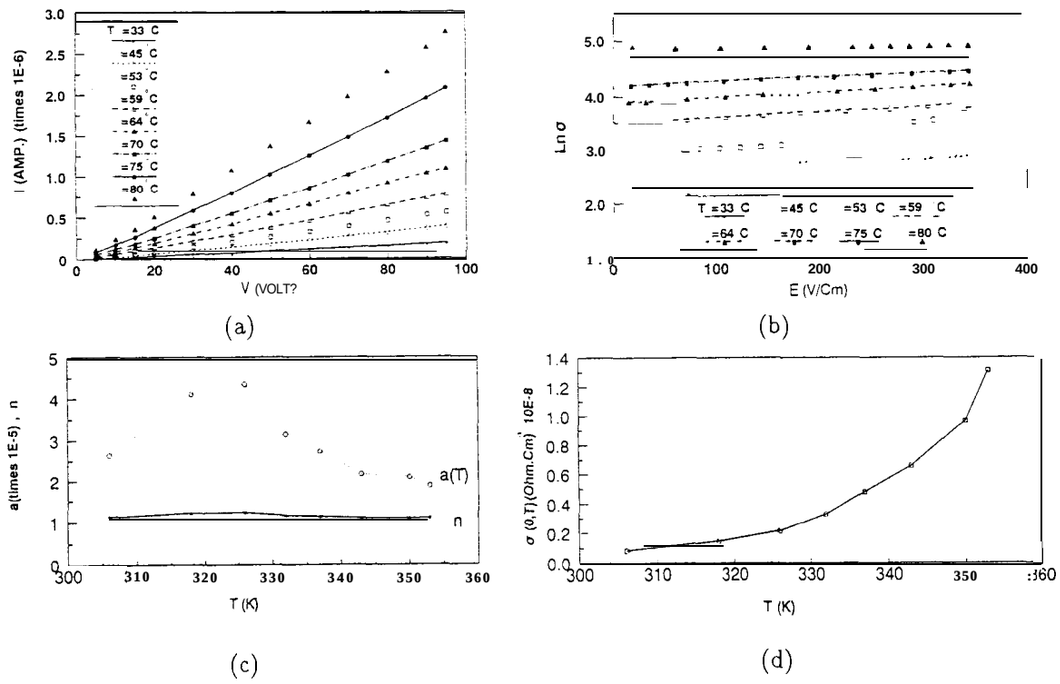

FIG. 2. (a) The current-voltage characteristics of bulk as-prepared sample of $Tl_{20}Ge_{14}Se_{66}$ composition at different temperatures.
(b) The Ln σ Vs E(V/cm) plots for the as-prepared composition at different temperatures.
(c) Temperature dependence of the power n and the characteristic length a(T) cm for the as-prepared composition.
(d) The dependence of $\sigma(0,T)$ (Ohm. cm)$^{-1}$ on the ambient temperature for the as-prepared composition.

values for T and high range of E can be attributed to the fits being taken over the whole range of E. However, such slight deviation of n from the value unity and its almost independency on T characterize weak possibility of field enhancement of the electrical conductivity and this enhancement is weakly activated by the temperature of measurements especially in the range below T_g.

For the as-prepared composition (within the non-ohmic region) the field dependence of the electrical conductivity at different ambient temperatures was as shown in Fig. 2(b) where the plots of $\ln\sigma$ vs E are linear with plus sign coefficients. From the first glimpse, these linear plots seem as good fits of the model proposed by Marshall and Miller [14] which suggests that at fixed temperature T, the field dependence of the electrical conductivity can be described by the following formula

$$\sigma = \sigma(0,T) \exp(e\ a(T)E/KT), \tag{2}$$

where e is the electronic charge and K is the Boltzmann's constant. Both the zero-field conductivity $\sigma(0,T)$ and the temperature dependent characteristic length $a(T)$ changed with T as shown in Figs. 2(c) and 2(d) respectively. As it is seen, within the range of E (18-350 Vcm^{-1} where the enhancement of σ is possible, the temperature dependent characteristic length $a(T)$ increases with increasing T possessing a maximum value at 53 °C. Then, it falls almost monotonically with further elevation of T. Besides, within the considered range of T (30-80 °C), values for $a(T)$ between $(2\text{-}4.5)10^{-5}$ cm coud be obtained. On the other hand, as it is seen on Fig. 2(d), the zero-field electrical conductivity $\sigma(0,T)$ obtained from the extrapolations of ln σ vs E plots shown on Fig. 2(b) increased continuously with increasing T.

Annealing of bulk samples was carried out at fixed temperatures in the range 80-150 °C for 1h. The temperature of annealing was elevated in steps of 5 °C. This narrow step in the variation of the temperature of annealing is because of the high sensitivity of the structural changes in the composition to the isochronic annealing. Moreover, measurements of the $I-V$ characteristics were carried out while the sample was kept at the temperature of annealing (i.e. not after cooling to the room temperature as usual.). This might have the advantage of revealing the role of annealing (instantaneously) at the process of annealing itself. As it is shown on Figs. 3(a) and 3(b) the $I-V$ characteristics are non-linear as for the case of as-prepared composition where measurements were carried out at different environmental temperatures in the rang 33-80 °C which are below those considered for annealing $80 \geq T_{an} \leq 150$ °C. Comparison beween Figs. 2(a) and 3(a) and 3(b) indicates that, the role of elevating T in the range 33-80 °C and T_{an} in the range 80-150 °C is similar in feature. Both resulted in an increase of the isovoltage current and so, enhancement of the electrical conductivity. Despite of this isochronic annnealing, the double logarithmic relations between (J) and (E) were linear emphasizing the validity of Eq. (1). Further, values of the power (n) changed with T_{an} as shown on Fig. 3(e). Comparison between plots on Figs. 2(c) and 3(e) reveals that the role of T_{an} on n is significent. While n seemed almost independent on T, it possessed maximum at $T_{an} = 110$ °C and increased abruptly at $T_{an} \geq 140$ °C, possessing anomalously high value at $T_{an} = 145\text{-}150$ °C which may have a special significance. Regarding the XRD on Fig. 1, the maximum for the power n observed at 110 °C is probable to be due to the start of nucleation and crystallization process. The almost independent region of n ($T_{an} \sim 120-140$ °C) may be due to that within this range, nucleation of new phases continues and does not be associated with appreciable increase in the intensity of crystallization. On the other hand, annealing resulted in promotion of the values of n which reveals stronger field enhancement of the electrical conductivity.

As for the as-prepared condition, the plots of ln σ vs E at the different temperatures of annealing were all linear as shown on Figs. 3(c) and 3(d). The linear fits of Eq. (2) gave values for $a(T)$ and $\sigma(0,T)$ changed with T_{an} as shown an Figs. 3(e) and 3(f) respectively. As it is seen in Fig. 3(e), the dependence of $a(T)$ and n on T_{an} are identical in feature. As for n, $a(T)$ possessed maximum at the temperature of annealing 110 °C which is almost equal to the glass transition temperature and extremely high values at the temperatures of annealing < 140 °C. On the other hand, comparison between the values for $a(T)$ for as-prepared (Fig. 2(c)) and annealed (Fig. 3(e)) it is obvious that, the latter are lower by about one order of magnitude. This may be due to that, despite the annealed sample

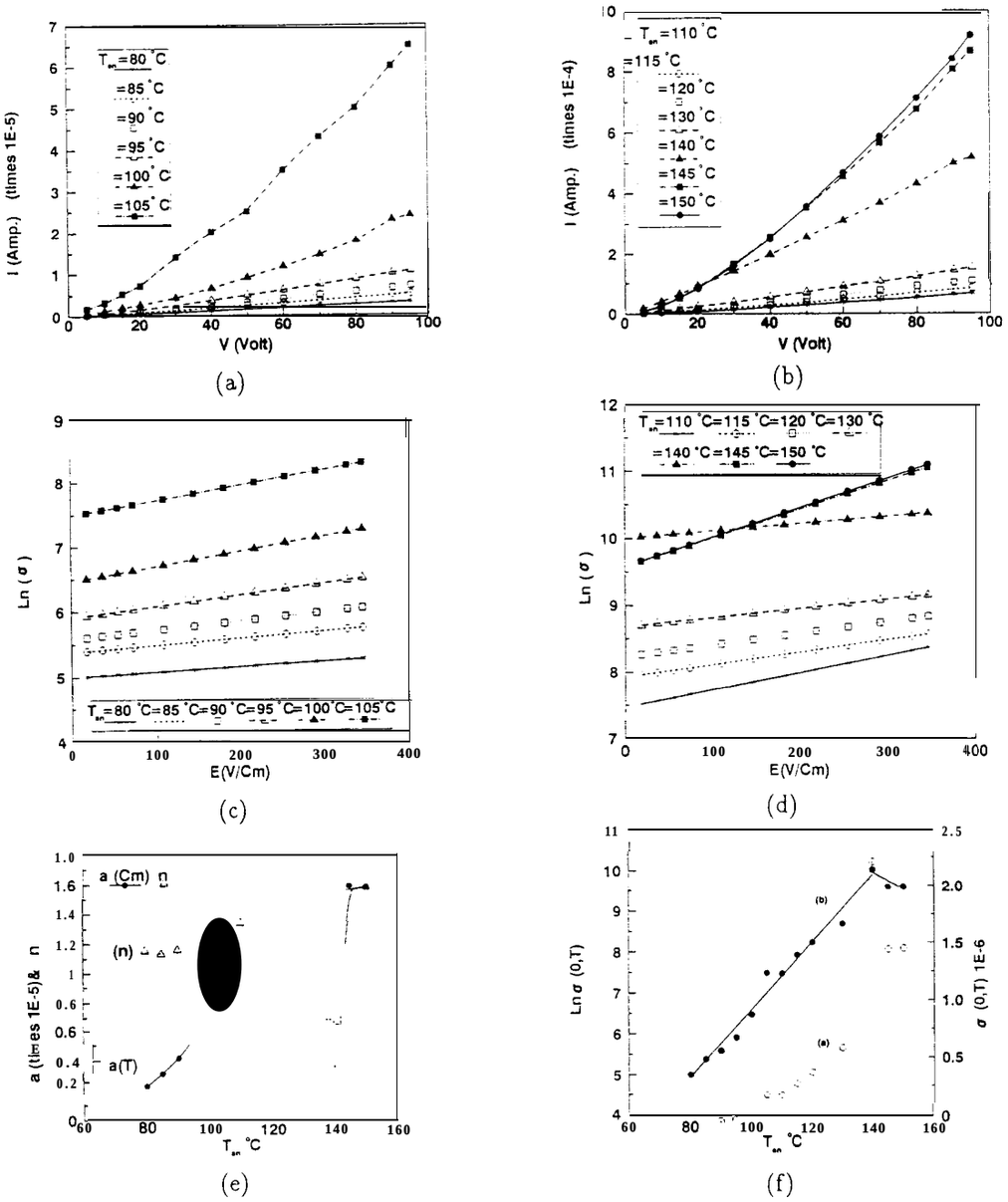

FIG. 3. (a) & (b) The Current-Voltage Characteristics at different temperatures of annealing of the composition $Tl_{20}Ge_{14}Se_{66}$.
(c) & (d) Relation between Ln (σ) and E(V/cm) at different temperatures ofannealing.
(e) The dependence of n and a(T) on the temperature of annealing.
(f) Relation between (a) σ and (b) $\mathrm{Ln}\,\sigma(0,T)$ on the temperature of annealing.

is consisting of different species of phases together which may result in shortening of the characteristic length, the sample is comparatively more homogeneous. A contradictory observation is, $a(T)$ increased with increasing the temperature of annealing. This can be due to the separation of Tl *as* an elemental phase in the sample.

On the other side, the zero-field conductivity $\sigma(0,T)$ showed dependence on T_{an} *as* shown on Fig. 3(f). In the range $T_{an} \leq$ **140** °C, the dependence of $\sigma(0,T)$ on T_{an} seemed typically similar to that for the as-prepared condition Fig. 2(d). In the range $T_{an} \geq$ **140** °C, $\sigma(0,T)$ decreased sharply to possess a stable value at T_{an} **= 145** and 150 °C. This confirms the data obtained from the XRD analysis Fig. (1), where annealing at 140oC was associted with separation and appreciable crystalliztion of different species of phases. These different phases existed together might result in shortening in the mean free pathof the charge carriers which can result in a decrease of the electrical conductivity. The situation seems to some extent contradictory because of the possible confusion between **a(T)** and the mean free path since **a(T)** increased sharply with elevating T_{an} above 140oC. The confusion may be withdrawn, since **a(T)** is related to the hopping characteristic length. As it is seen from XRD diffractograms on Fig. 1, annealing at 140oC was associated with not only phase separation but also crytallization. The existence of different phases means, the sample became polycrystalline. Although it can contribute to more ordering, it can contribute also to dishomogeneity of the sample. However, either the samples were as-prepared or annealed, the values obtained for **u(T)** are higher by about two or three orders of magnitude with respect to those published 10-15Å for other chalcogenides [15-19]. The anomaly can be attributed to two main reasons: First; a compostion either as-prepared or thermally annealed is consisting of both amorphous and crystalline phases together as it can be revealed by XRD analysis Fig. 1. Second; the considered range of the applied electric field is about three orders of magnitude lower than that needed to fit well Eq. (2).

Fig. 4(a) shows the possibility of thermal activation of the DC electrical conductivity σ in the range ~ 30-80 °C at different temperatures of annealing 95-150 °C. The plots between $\ln\sigma$ vs l/T are linear. However, each of the plots is consisting of two parts separated at certain temperature (T_r) indentified from the extrapolation of the normal to the abscissa from the meeting point of the linear fits of the two linear parts) which is dependent on the temperature of annealing. For the temperatures of annealing in the range 100-130 °C, while the range below T_r is characterized by semimetallic behaviour and σ decreased with increasing **T,** the range above **T,.** is characterized by a normal semiconductor behaviour and σ increased with increasing **T.** For T_{an} **=** 130 °C, the range above T_r **was** characterized by gapless-like semiconductor behaviour and σ showed almost independency on T. For T_{an} = 95 °C and ≥ 145 °C, the behaviour extended that of semiconductor over the whole range of **T.** The temperature of transition (T_r) is very sensitive to the temperature of annealing as shown in Table I.

As it is seen in this table, where (T_r) represents semiconductor-semiconductor transition, it decreased continuously with elevating T_{an} from 140 to 150 °C. In contrase, except for T_{an} **=** 100 °C, where T_r represents semimetal-semiconductor transition, it increased continuously with increasing T_{an} from 105-120 °C. However, for the two temperatures of annealing 120 and 130 °C, T_r possessed the same value. Such behaviour emphasizes the corresponding structural changes with the process of anneaing.

Within the semiconducting region, the following usual equation was applied to de-

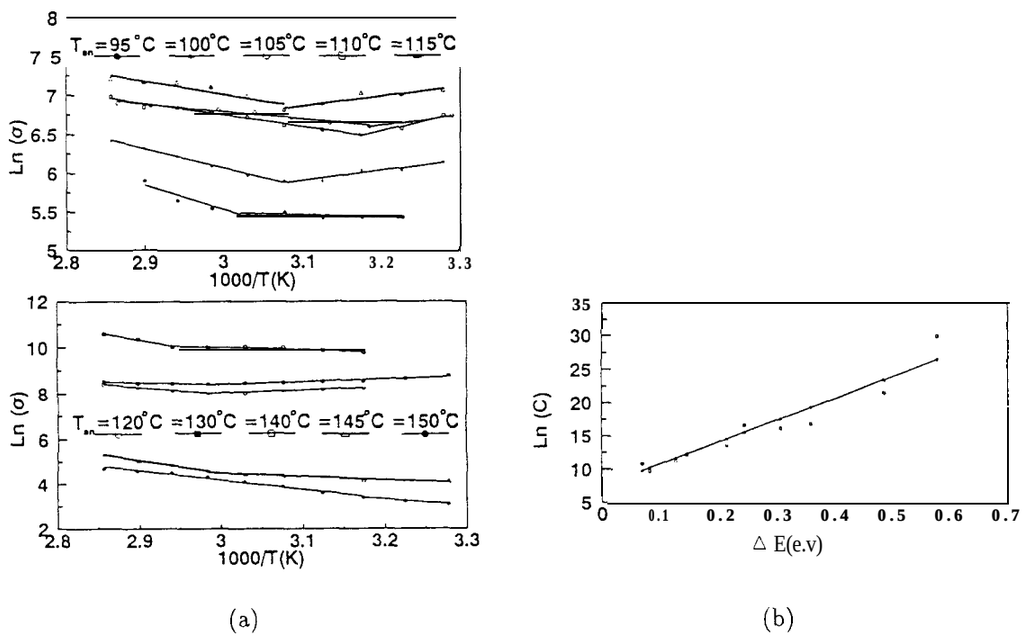

(a) (b)

FIG. 4. (a) the relation between Ln σ and 1000/T(K) at different temperatues of annealing. (b) MN Rule, striaght line fitting by using Least-Squar method where • I Exp. and □ calculated.

TABLE I. Dependence of the temperature of transition (T_r) on the temperature of anealing (T_{an}).

Semiconductor-Semiconductor Transition		Semimetal-Semiconductor Transition	
T_{an}	T_r	T_{an}	T_r
95	59.226	100	52.733
140	66.789	105	41.465
145	61.784	110	42.457
150	42.457	115	49.581
		120	62.008
		130	62.008

scribe the thermal activation of the electrical conductivity where,

$$\sigma = Ce^{-\Delta E/KT}. \tag{3}$$

Where C is the pre-exponential or the temperature independent electrical conductivity. Its value at a certain temperature of annealing was calculated from the extrapolation to (l/T) = 0 on the $\ln\sigma$ axis. Accordingly [20], the pre-exponential C equals $\sigma_0 e^{(\gamma/k)}$ and $\sigma_0 = e\mu_h g(E_v)KT$ where σ_0 is the minimum metallic conductivity, γ is the temperature dependence of the band gap, K is the Boltzmann ' s constant, e the charage on holes, μ_h the mobility of the holes, g(Ev) the density of states per unite energy at the mobility edge and T the absolute temperature.

Therefore Eq. (3) can be entirly rewritten as follows

$$\sigma = \sigma_0 e^{\gamma/K} e^{-\Delta E/KT} = e\nu_h g(E_v)KTe^{\gamma/K} e^{-\Delta E_0/KT}. \tag{4}$$

It is obvious that, σ_0 includes the charge carrier mobility and density of states. In addition, accordingly [21], the activation energy AE is a function of the electronic energy levels of the chemically interacting atoms in the glass and, hence, of energy band gap. In Eq. (3), the pre-exponential C and the activation energy AE both obtained at the same temperature of annealing were plotted against each other as shown in Fig. 4(b). As it is seen, the semilogarithmic plot is linear reflecting a relation between C and AE typically as that known by the Meyer-Neldel (MN) rule. Accordingly [22], the dependence of the pre-exponential C on the activation energy AE can be formuluted empirically

$$C = C_0 e^{\Delta E/M} \tag{5}$$

or

$$\ln C = \ln C_0 + (1/M)\Delta E$$

Where C_0 and M are constants. While both C and AE are dependent on the temperature of annealing, the constants C_0 and A4 seemed satisfactory to cover all the range considered for the temperature of annealing on condition that the behaviour within this range still that of semiconductor. However, it has to be stated that, the MN rule is an empirical relation which is usually observed in electronically, polaronically, and ionically conduction solids [23]. Besides, such observed dependence of C on AE may reveal a possibility of variation of the mobility of the charage carriers with the temperature of annealing.

In the range below T_r which is a matter can be determined from Table I where the behaviour was that of semimetals, the double logarithmic relation of the resistivity vs temperature at different annealing tmperatures ($100 \leq T_{an} \leq 130$ °C) were linear as shown in Fig. 5. Despite, the allowed temperature range is very narrow, these linear plots can suggest a power relation to describe the temperature dependence of resistivity as follows

$$\ln\rho = \ln B + m\ln T$$

or

$$\rho = B + T^m \tag{6}$$

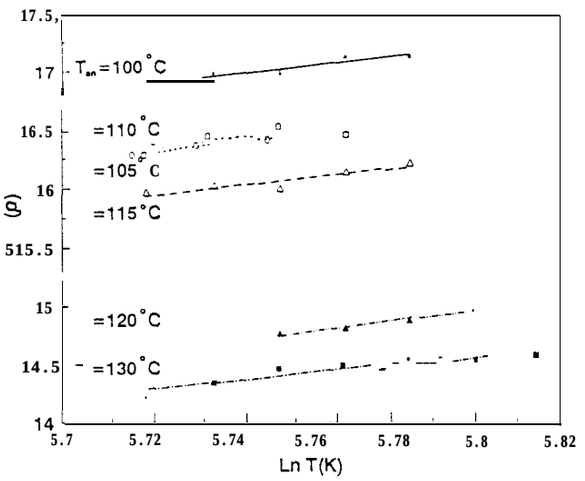

FIG. 5. Temperatue dependence of resistivity at different annealing temperatures within the semimetallic region.

TABLE II. Variation of both B and m on the temperature of annealing.

$T^{\circ}_{an}C$	100	105	110	115	120	130
ln B	-5.573	-7.034	-5.2097	-6.082	-11.52	-6.83
B 10^3	3.8	.88	5.46	2.28	.01	1.07
m	3.929	4.082	3.7685	3.8516	4.5665	3.649

Both the extrapolation B and the power m where calculated with their dependence on the temperature of annealing as shown in Table II.

As it is seen in this table, the power m changed with T_{an} in an oscillatory manner. However, its lowest values were attained at 110 and 130 °C of annealing. Besides, all values obtained for the power m are not coincided with those typically known for the pure metals which are typically equal to unity and 5 at high and low temperature range with respect to Debye temperature [24]. Similar results have been obtained for BiSb composition [25]. Similarly this semimetallic behaviour in the present composition may support the view that the anharmonicity of the lattice potential increases with increse of temperature which in turn, enhance the process of scattering, a matter results in causing a rise in ρ with increase of T. The oscillatory change of the power m with the sequential increase of T_{an} may be due to a corresponding oscillatory phase separation and crystallization which in turn is an oscillatory change in the composition stoichiometry. That is because the stoichiometric

composition contributes to reduction of resistivity and due to the violation of potential periodicity would be recovered. Thus, the degree of anharmonicity will be reduced. Besides, the X-ray diffraction analysis indicated that the annealed samples are containing of both amorphous and crystalline phases together, irrespective of the temperature of annealing. Nevertheless, as it is seen also from the XRD analysis, annealing results in separation of different phases with their intensities increase with increasing the temperatures of annealing, a matter expected to enhance the violation of the potential which can strogly result in more scattering and that rapid increase of ρ with T. The limitation of this semimetallic behaviour within a certain range of T (below T_r) and the dependence of T_r on the temperature of anealing makes the behaviour quite different from that of pure metals. In addition, in the latter, the concentration of the free electrons is independent on temperature and all the change in ρ is resulting from the change in the carriers mobility. Thus, within this range of T, the inhibition in conductivity may be resulting from inhibition of mobility and reduction in the mean free path due to more concentration of the defects and scatering centres. Besides, due to the presence of several charge carrier groups with different effective masses, electron-electron normal scattering process might also contribute to resistivity [26]. Morever, the T^n dependence f resistivity was verified previously and it is suggested to be associated with electron-phonon resistivity [24]. However, such semimetallic behavioure could be obseved for $TlCo_2S_{1.0}Se_{1.0}$ in the range below the room tempertaure [27]. Meanwhile, they confirmed that, solid solutions with the formula $TlCo_2S_XSe_{2-X}$ are highly metallic with small room temperature resistivity. These solid solutions and other related materials are fairly typical of metallic materials which undergo magnetic ordering [28,29-32]. The drop in resistivity as the temperature exeeds certain value is attributed to a decrease in conduction electron scattering by the paramagnetic ions as their spins become progressively correlated upon magnetic ordering. Since, the semimetallic behaviour can be viewed as a result of overlapping of valence and conduction band [8,13,26,33-34] which is a matter in turn affected by various factors such as the degree of homogeneity, condition of annealing and the range of temperature of measurements, thus, the variations of the power m and the trasition temperatue T_r with T_{an} are expected.

As it is seen from the X-ray diffractograms on Fig. 1, the sturcture is entirely amorphous for the as-prepared composition and even the temperature of annealing was raised to $\sim$ 110 °C where very weak separated phases could be observed. Above $T \sim 110$ °C the composition is having a polycrystalline structure.

Therefore, at all considered temperatures of annealing ≥ 90 °C a sample can be considered to contain both amorphous and crystalline phases together. Thus, according to Mott's model [35], the electrical conductivity can be considered as a sum of σ_{ext} (bandtype conductivity) and σ_{hop} (due to hopping conduction within the localized states). The Mott's formula for the hopping conductivity and its temperature dependence is given by

$$\sigma = \frac{\sigma_0}{\sqrt{T}} e^{(-T_0/T)^{1/4}} \tag{7}$$

Where

$$T_0 = \frac{18\alpha^3}{KN(E)}$$

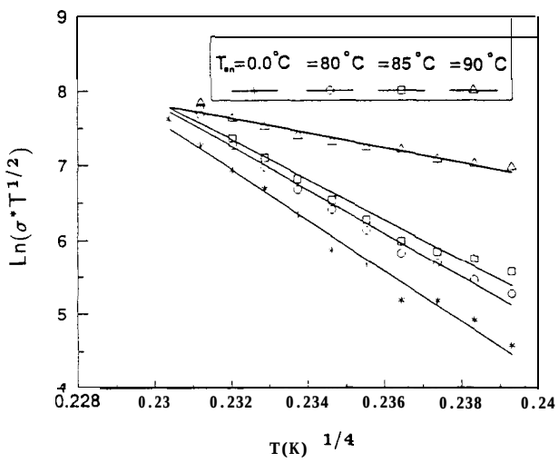

FIG. 6. The $T^{1/4}$ dependence of $\sigma T^{1/2}$ at different annealing temperatures.

$$\sigma_0 = \frac{N(E)}{2\pi\alpha K}\left(\frac{3e^2\mu\phi_0}{2}\right)^{1/2}$$

Where α is the inverse-fall-off length of the wave function of a localized state near the Fermi-Level to be 0.124 Å[33]. *N(E)* is the density of such states, μ is the typical phonon frequency and ϕ_0 is an overlap integral and is order of unity. On the oter hand, the average hopping distance (R) and hopping energy (W) are given respectively by the expressions

$$R = \left(\frac{9}{8}\frac{1}{\pi\alpha K N(E)T}\right)^{1/4} \tag{8}$$

$$W = \frac{3}{4}\frac{1}{\pi R^3 N(E)} \tag{9}$$

Fig. 6 indicates that, the experimental plots of $\sigma\sqrt{T}$ vs $T^{-1/4}$ at differnt temperatures of ealing ≤ 90 °C C fit good Eq. (7). This because up to the tmperature ~ 100 °C of anealing, the structure of the composition is still mainly amorphous, significant separation of crystalline phases could be observed when T_{an} exceeds ~ 100 °C. Despite of this mixed conducttion (extended band type and hopping between the loclized states) values of parameters $T_o, N(E), W$ and R were all calculated and their variation with the temperature of annealing was as shown in Table III.

As it is seen, the parameter (T_o) decreased drastically by about two orders of magnitude by elevating (T_{an}) just to 90 °C. Besides, such drastic decrease in T_o *was* sequential. The density of the localized states increased also sequentially with elevating the temperture of annealing. The parameter R decreased also consequential with elevating T_{an}. On the other side, W, except for $T_{an} = 80$ °C, decreased drastically with increasing T_{an} to 90 °C.

TABLE III. Variation of $T_0, N(E), W$ and R with the temperature of annealing in the range $T_{an} \leq 90$ "C.

T^{o}_{an}	$T_0(K)x10^8$	$N(E)$ $ev\,cm^3x10^{21}$	$R(cm)x10^{-8}$	W(mev)
0	137.0	1.09	6.45	0.82
80	75.60	1.97	5.21	0.86
85	5.429	2.75	4.78	0.80
90	1.030	145	1.77	0.30

Despite values on N(E) are coincided well, those for T_o are higher and those for R and W are lower by about two orders of magnitude with those obtained for other chalcogenide compositions [21,34].

IV. Conclusion

Either the bulk samples of $Tl_{20}Ge_{14}Se_{66}$ were as-prepared or isochronically annealed at different temperatures, the $J-E$ characteristics could be described by powerform equation, even the characteristics were measured at different environmental and could be described by an exponential equation. In addition to that, $a(T)$ is strongly dependent on both T and T_{an}; annealing inhibits its values by about one order of magnitude. The Zero-field conductivity showed possibility of thermal activation. The band-type activation energy changed with the pre-exponential conductivity according to the Meyer-Neldel rule. Because of the complicated internal structure, semimetallic, band-type and hopping conduction behaviours could be all observed. Domination of certain type of conduction is a matter depends on both the environmental and annealing temperatures.

References

[1] R. M. Mehra, Radhey Sham and P. C. Mathur, Phys. Rev. B19, 6525 (1979).
[2] C. A. Maji, Phil. Mag. **B49, 1 (1984).**
[3] K. Arai, T. Kuwahat, H. Namikawa, and S. Saito, Jpn. J. Appl. Phys. **11, 1080 (1972).**
[4] M. Zope, B. D. Muragi, and J. K. Zope, J. Non. Cryst. Solids 103, **195 (1988).**
[5] B. D. Muragi and J. K. Zope, Ind. J. Pure and Appl. Phys. communicated.
[6] D. Ader, H. K. Henisch, and N. F. Mott, Rev. Mod. Phys. 50, 209 (1978).
[7] B. D. Murgi and J. K. Zope, Ind. J. Pure and Appl. Phys. 25, 77 (1987).
[8] N. F. Mott and E. A. Davis, *Electronic Processes in* Noncrystalline *Materials* (Clarendon Press, Oxford, 1971), Chap. 1.
[9] H. Fritzsche, in *Proc. Seventh Int. Conf. on Amorphous and Liquid Semiconductors,* ed. W. E. Spear (CICL, Univ. of Edinburgh, Scotland, 1977) p.3.
[10] S. R. Oshinsky, in Ref. [9], p.519.

[11] A. A. Andreev, Z. U. Borisova, E. A. Bichkov, and Y. G. Vlasov, in *Proc. Eighth Int. Conf. on Amorphous and Liquid Semiconductors,* Cambridge MA, August 27-31, 1979; J. Non-Cryst. Solids 35-36, 901 (1980).
[12] R. S. Street and N. F. Mott, Phys. Rev. Lett. 35, 1293 (1975).
[13] Nboru Tohge, Kimio Kanda, and Tsutomu Minami, Yogyo-Kyoka-Shi 94, 236 (1986).
[14] J. M. Marshall, and J. R. Miller, Phil. Mag. 27, 1151 (1973).
[15] P. W. Anderson, Phys. Rev. 109, 1492 (1958).
[16] T. C. Arnoldussen, R. H. Bue, E. A. Fagen, and S. J. Holmberg, Appl. Phys. 43, 1798 (1972).
[17] B. G. Bagley, Solid St. Commun. 8, 345 (1970).
[18] K. W. Boer and R. Haislip, Phys. Rev. Lett. 24, 230 (1970).
[19] M. H. Cohen, *Proc. on Semicond. Effects in Amorphous Solids* (Amsterdam, North Holland Publishing Co., 1970).
[20] N. F. Mott and E. A. Davis, *Electronic Processes in Non-Crystalline Materials,* 2nd ed. (Clarendon Press, Oxford, 1979).
[21] R. M. Mehra, Rajesh Kumar, and P. C. Mathur, J. Thin Solid Films 170, 16 (1989).
[22] W. Meyer and H. Neldel, Z. Tech. Phys. 12, *588* (1937).
[23] *G. G.* Roberts, J. Phys. C4, 3167 (1971).
[24] E. W. Fenton, J. P. Jan, A. Karlsson and R. Singer, Phys. Rev. 184, 663 (1969).
[25] M. M. Ibrahim, E. KH. Shokr, M. M. Wakkad, and N. M. Megahed Ind. J. of Pure and App. Physics. 27, 181 (1989).
[26] W. G. Baren, Proc. R. Soc. A(GB) 158, 383 (1937).
[27] Mark Greaney, Guohe Huan, K. V. Ramanujachary, Zeri Teweldemedhin and Martha Greenblatt, J. Solid State Commun. 79, 803 (1991).
[28] K. S. V. L. Narasimhan, V. U. S. Rao, R. L. Bergner, and W. E. Wallace, J. Appl. Phys. 46, 495 (1975).
[29] G. Huan, M. Greenblatt, and M. Croft, Eur. J. Solid State Inorg. Chem. 26, 193 (1989).
[30] G. Huan, M. Greenblatt, and K. V. Ramanujachhary, Solid State Commun. 71, 221 (1989).
[31] A. R. Newmark, G. Huan, M. Greenblatt, and M. Croft, Solid State Commun. 71, 1025 (1989).
[32] G. Huan and M. Greenblatt, J. Less-Common Metals 156, 247 (1989).
[33] H. Fritsche, in *Amorphous and Liquid Semiconductors,* ed. J. Tauc, (Plenum, London, 1974) p.221.
[34] M. M. Ibrahim and M. N. Abd El-Rahiem, Physica Scripta. Vol. 38, 762-767, (1988).
[35] N. F. Mott, J. Non-Cryst. Solid 8-10, 1 (1972).